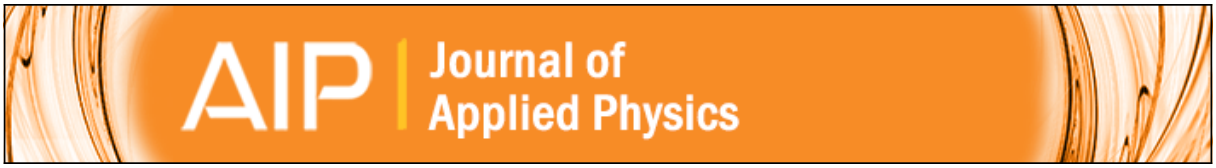

The effects of nitrogen profile and concentration on negative bias temperature instability of plasma enhanced atomic layer deposition HfO x N y prepared by in situ nitridation

W. J. Maeng and Hyungjun Kim

Citation: Journal of Applied Physics **104**, 064111 (2008); doi: 10.1063/1.2978360
View online: http://dx.doi.org/10.1063/1.2978360
View Table of Contents: http://scitation.aip.org/content/aip/journal/jap/104/6?ver=pdfcov
Published by the AIP Publishing

The effects of nitrogen profile and concentration on negative bias temperature instability of plasma enhanced atomic layer deposition HfO_xN_y prepared by *in situ* nitridation

W. J. Maeng and Hyungjun Kim[a)]
Department of Materials Science and Engineering, Pohang University of Science and Technology (POSTECH), San 31, Hyoja-Dong, Nam-Gu, Pohang 790-784, Republic of Korea

(Received 2 June 2008; accepted 17 July 2008; published online 22 September 2008)

We have prepared plasma enhanced atomic layer deposition HfO_xN_y thin films by *in situ* nitridation using nitrogen/oxygen mixture plasma and studied the effects of nitrogen contents and profiles on the negative bias temperature instability (NBTI). The nitrogen depth profiles and concentrations were controlled by changing the exposure sequences and the nitrogen to oxygen flow ratio, respectively. The best immunity to NBTI degradations was obtained for the nitrogen to oxygen ratio of 2:1 when nitrogen atoms are incorporated away from the high k/Si interface. We propose a dielectric degradation mechanism based on the reaction-diffusion model in which nitrogen plays a role of hydrogen generator at the interface and diffusion barrier in the bulk film. © *2008 American Institute of Physics*. [DOI: 10.1063/1.2978360]

I. INTRODUCTION

The negative bias temperature instability (NBTI) has been considered as one of the key limiting factors for the device scaling, resulting in the instability of threshold voltage (V_{th}) and creating interface states.[1] It occurs primarily in p-channel metal-oxide-semiconductor field-effect transistors (MOSFETs) with negative gate voltage bias and appears to be negligible for positive gate voltage and for either positive or negative gate voltages in n-channel MOSFETs.[2] Reaction-diffusion (RD) model of NBTI suggests that the hydrogen desorption at the interface is responsible for the dielectric degradation in lower stress voltages than Fowler–Nordheim regime.[3,4] The hydrogen atoms at the interface, which are incorporated during fabrication procedures such as forming gas annealing (FGA), make bonds with Si dangling bonds at the interface, which results in the reduction in the interface state density. However, under the constant voltage stress at elevated temperature, the hydrogen-silicon bonds are broken and hydrogen atoms are released. By this, interface states as well as trap charges are generated, leading to NBTI.

While the incorporation of nitrogen atoms to gate oxide produces beneficial effects, such as the reduction in leakage currents and improvements of the reliability by passivating oxygen vacancy states and enhancing structural stability, an early study on ultrathin SiO_2 gate oxide has shown that excess nitrogen incorporation at the interface accelerates device degradation through NBTI. The exacerbation of NBTI by interface nitrogen atoms for thin SiO_2 gate oxide was attributed to the enhancement of hydrogen trapping reaction due to lower reaction energy for Si–N than Si–O, resulting in the increase in both interface states and positive fixed charges.[5,6] Thus, for prenitridation process leading to high nitrogen concentration at the interface, the gate oxide is continuously degraded with nitrogen concentrations.[7,8] Meanwhile, other studies reported positive effects on NBTI by nitrogen incorporation near the gate.[9] Also, there was another report that low nitrogen content improves the reliability, while larger content accelerates the degradation under NBT stress conditions.[10]

Thus, we infer that nitrogen depth profiling to produce low nitrogen incorporation at interface and proper amount of nitrogen incorporation is important for producing gate oxide with immunity for NBTI. For example, Ang *et al.*[11] showed that the plasma nitridation, resulting in the nitridation at the top of the gate oxide, produces more resistance to NBTI than thermal nitridation. However, systematic study on the nitrogen incorporation on NBTI according to nitrogen profile and concentration has been rare. Similar to SiO_2 gate oxide, NBTI has been identified as a serious reliability issue for devices using high k gate oxide as well.[3,12] Although it is generally accepted that hydrogen plays a central role as for thin SiO_2 gate, not many studies have been carried out on the effects of nitrogen incorporation for NBTI of devices with high k gate oxide.

Recently, we reported the nitrogen depth profile control by *in situ* nitrogen incorporation during plasma enhanced atomic layer deposition (PE-ALD) HfO_2 thin films using nitrogen/oxygen mixture plasma.[13] The electrical and the interface properties were significantly improved when the nitrogen atoms are located in the middle of the HfO_2 films. However, the effects of nitrogen concentration of depth profile controlled HfO_xN_y was not studied. Especially, the *in situ* nitridation process during PE-ALD has benefits to produce high k films with atomically controlled nitrogen profile, which is suitable to produce an ideal model system for studying the effects of nitridation on the NBTI degradation. Here, we report the effects of nitrogen concentration and nitrogen profile for enhancing dielectric reliability, focusing on the role of nitrogen on NBTI of high k. We found the existence of optimum nitrogen concentration regarding NBTI degrada-

a)Electronic mail: hyungjun@postech.ac.kr.

tion. Based on these results, we discuss the NBTI mechanism for nitrogen incorporated high k gate oxide.

II. EXPERIMENTAL PROCEDURE

A home-made remote PE-ALD system was used in this study. Tetrakis(dimethylamino)hafnium (TDMAH) was used as a Hf precursor. First, to study the effects of nitrogen depth profile, the samples with different nitrogen depth profiles, bottom (BN), middle (MN), and top plus middle (TMN) nitrided samples, were prepared by changing the sequence of O plasma and N/O mixture plasma with the N/O flow ratio fixed at 2. The total number of growth cycles was 30 for each sample. 20 cycles with O plasma and 10 cycles with N/O mixture plasma as a reactant were used for MN and BN samples. In contrast, the TMN sample was prepared by 10 cycles of O plasma followed by 20 cycles of N/O mixture plasma as reactants. Next, to study the effects of nitrogen concentrations, TMN samples with different nitrogen concentrations were prepared by changing the $F_{N/O}$ (N/O flow ratio). Typical HfO_2 or HfO_xN_y ALD sequence was composed of TDMAH exposure time of 1.5 s, plasma reaction time of 3 s, and purging time of 5 s between those. The oxygen and nitrogen gases were flown into a rf plasma source, which consists of a quartz tube wrapped with a multiple-turn coil set at 13.56 MHz providing a power level of up to 600 W. For the current experiments, the flow of oxygen, controlled by Mass Flow Controller (MFC), was 20 SCCM (SCCM denotes cubic centimeter per minute at STP) and the plasma power was 300 W. The chamber was purged by 75 SCCM Ar gas between precursor and reactant exposure step.

The films were deposited on p-type Si (001) substrates, which were cleaned at 70 °C for 10 min in RCA solution [1:1:5 (v/v/v) $NH_4OH/H_2O_2/H_2O$] followed by dipping in buffered oxide solution for 30 s to remove native oxide. For MOS capacitor fabrication, Ru was deposited by magnetron sputtering as a gate metal through patterned shadow mask. Also, thermal evaporated Au was used as a back contact. Postdeposition annealing and FGA were carried out at 400 °C for 10 min in oxygen environment and for 30 min in $H_2$5%–$N_2$95%, respectively, to reduce trap charges. Capacitance-voltage (C-V) and current-voltage (I-V) characteristics were determined by using Keithley 4200 semiconductor parameter analyzer with HP4284 LCR meter. The capacitors were swept from inversion (+2.5 V) to accumulation (−2.5 V) and back to check the amount of C-V hysteresis.

Positive charge density (N_p) was determined by V_{FB} shift from ideal V_{FB}. We assumed that the ideal V_{FB} is 0 V due to the p-type Ru gate used. Also, the interface state density (D_{it}) was determined by conductance method carried out at various frequencies from 1 kHz to 1 MHz. Conductance G_p versus voltage and frequency was measured. Measured G_p value was corrected by taking into account series resistance and insulator capacitance.[14] Also, conductance loss (G_p/ω) was selected at maximum value in swept voltage. The D_{it} value was extracted by the following equation:[15]

$$D_{it} = \left(\frac{G_p}{\omega}\right)_{max} [qf_D(\sigma_s)A]^{-1}, \quad (1)$$

where G_p/ω is the corrected conductance loss, ω is the angular frequency ($\omega = 2\pi f$, f is the measurement frequency), q is the electronic charge (1.6×10^{19} C), f_D is the universal function as a function of standard deviation of band banding σ_s, and A is an area of metal gate. For HfO_2, the f_D is 0.35–0.4.[15] To study the NBTI characteristics, the −3 V voltage stress was applied for 3 min at room temperature (RT) to 125 °C. After the voltage stresses, the V_{FB} shift and the variations in D_{it} were measured.

III. EXPERIMENTAL RESULTS

First, we studied the effects of nitrogen profile on NBTI by measuring the flat band voltage shift (V_{FB}) and D_{it} of samples with nitrogen to oxygen flow ($F_{N/O}$) of 2 at 125 °C. Figure 1(a) shows that that the initial V_{FB} of BN sample has a significant negative shift (−0.3 V), which can be explained by high nitrogen concentrations at the interface for BN nitridations. After voltage stress, V_{FB} is further shifted to negative direction due to additional positive charge generation in dielectric thin film. From the equation $\Delta N_P = -C_{ox}\Delta V_{FB}/q$, the trapped positive charge density change (ΔN_p) was calculated for BN, MN, and TMN samples [Fig. 1(b)]. The ΔN_p of MN sample after 5 min stress is about 1.2×10^{13} cm^{-2},which is about two times smaller than that of BN, while TMN sample has the least amount of charge generation.

Figure 1 also shows the absolute values and changes in interface state density change (ΔD_{it}) of BN, MN, and TMN samples as a function of stress time at 125 °C. Figure 1(c) indicates that the initial interface state density of BN has the highest value (3.0×10^{12} eV^{-1} cm^{-2}), while MN (1.3×10^{12} eV^{-1} cm^{-2}) and TMN (9.4×10^{11} eV^{-1} cm^{-2}) have lower values than untreated HfO_2 (2.4×10^{12} eV^{-1} cm^{-2}) sample. In addition, the interface state density change (ΔD_{it}) of MN is about $1.3\times$ x 10^{13} cm^{-2} eV^{-1}, which is three times lower than that of BN. Meanwhile, the ΔD_{it} values of the MN sample are higher than those for TMN. Thus, the TMN sample has the best electrical properties in terms of reliability depending on voltage stress at elevated temperature. For the BN sample, most of nitrogen atoms are incorporated into interface region in contrast to MN and TMN samples. Thus, the fast degradation of BN sample shown in Fig. 1 can be explained by the RD model, in which the degradation is enhanced by high interface nitrogen content.

To study the effects of nitrogen concentration on the electrical properties, TMN sample with different nitrogen concentrations were prepared by changing $F_{N/O}$ from 0.5 to 9. The nitrogen concentrations, determined by X-ray photoelectron spectroscopy (XPS), increased from 1 at. % for $F_{N/O}=0.5$ to 5.5 at. % for $F_{N/O}=9$. We have compared the electrical properties of TMN HfO_xN_y samples with $F_{N/O}=0.5$, 1, 2, and 4 measured at room temperature. Figure 2(a) shows the C-V characteristics of TMN samples with different nitrogen concentrations. The capacitance equivalent thickness (CET) values were slightly different among these

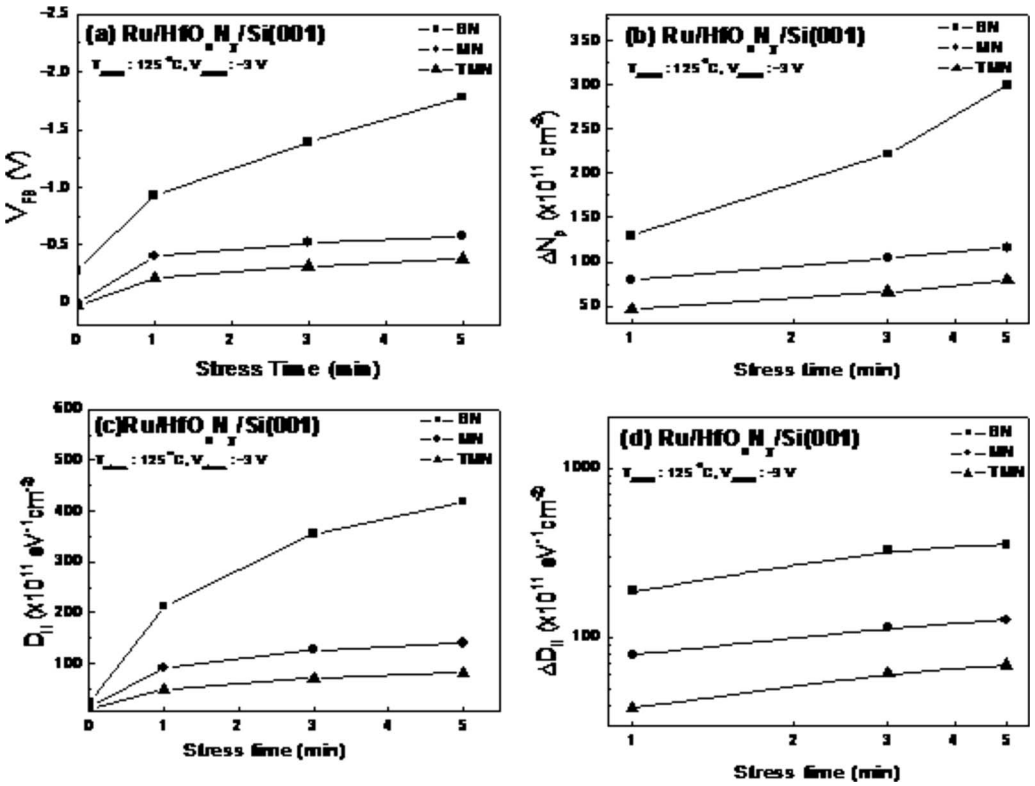

FIG. 1. (a) Measured V_{FB}, (b) change in trapped positive charge density (ΔN_p), (c) measured interface state density (ΔD_{it}), and (d) change in interface state density (ΔD_{it}) of BN, MN, and TMN samples as a function of stress time under −3 V of constant voltage stress at 398 K.

samples (1.15 nm for $F_{N/O}$=0.5, 1.12 nm for $F_{N/O}$=2, and 1.10 nm for $F_{N/O}$=4). The reduction in CET value with increasing $F_{N/O}$ is a general observation caused by the increase in dielectric constant with N incorporation. For example, it was reported that 5% N incorporation in HfO_2 films increases the dielectric constant about 17%.[16] In addition, a noticeable V_{FB} shift (−0.8 V) was observed for sample with $F_{N/O}$=4 with significant hysteresis (~0.2 V). Meanwhile, the V_{FB} shift and the hysteresis values (−0.25 and ~0.08 V, respectively) were almost identical for samples with $F_{N/O}$ =0.5 and 2. The large hysteresis and V_{FB} shift for sample with large nitrogen concentration indicates significant generation of positive charges and trap charges. The positive charges can induce the hysteresis and V_{FB} shift by large nitrogen incorporation near interface. Also, the trap charges can be induced from nitrogen related species such as N_2 or N–O by large amount of nitrogen for N/O mixture plasma ($F_{N/O}$>)2 leading to the hysteresis due to charge trapping and detrapping near interface.[17]

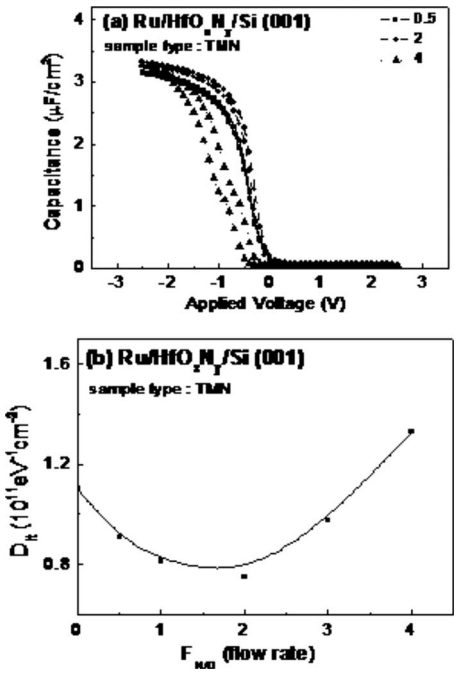

FIG. 2. (a) The capacitance-voltage curves of TMN samples prepared with $F_{N/O}$=0.5, 2, and 4, and (b) the interface state density (D_{it}) as a function of $F_{N/O}$.

Figure 2(b) shows the D_{it} values of these samples obtained by conductance method. For $F_{N/O}$<2, the D_{it} values decrease with increasing $F_{N/O}$. In contrast, the D_{it} values increase for $F_{N/O}$>2, with minimum value of 0.8×10^{11} eV^{-1} cm^{-2} at $F_{N/O}$=2. Thus, for the proper amount of the nitrogen incorporation, the interface state density can be reduced by passivating the dangling bonds at the interface.[18] For high nitrogen concentration, however, the nitrogen incorporation generates nitrogen related defects, leading to an increase in interface state rather than reducing it.[17] Similar interpretation can be applied for the dependency of nitrogen content on V_{FB} and hysteresis shown in Fig. 2(a).

Figure 3(a) shows N_p and ΔN_p, and Fig. 3(b) shows D_{it} and ΔD_{it} for TMN samples with different nitrogen concentrations after constant voltage stress (−3 V) for 5 min at RT. The film properties under Constant Voltage Stress (CVS) can

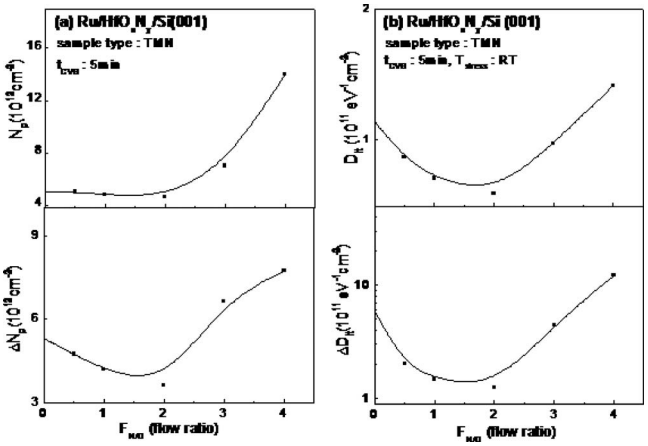

FIG. 3. (a) Change in trapped positive charge density (ΔN_p) with initial value of trapped positive charge density and (b) change in interface state density (ΔD_{it}) with initial value of interface state density as a function of $F_{N/O}$ for TMN sample after 5 min of voltage stress at RT with −3 V constant voltage stress.

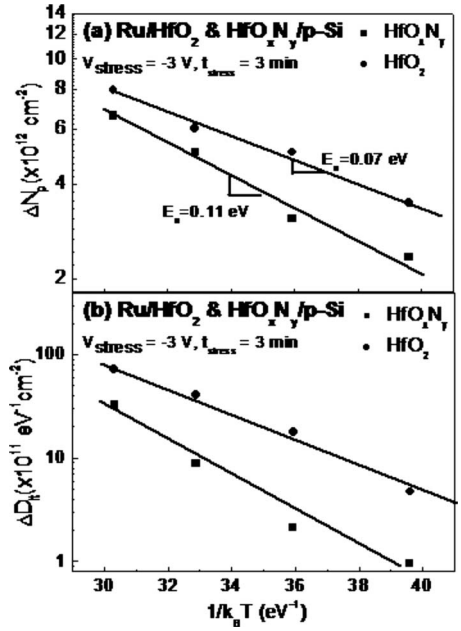

FIG. 4. (a) Arrhenius plot of the trapped positive charge generation (ΔN_p) and (b) ΔD_{it} after 3 min of voltage stress with −3 V stress for HfO_2 and TMN sample prepared at $F_{N/O}=2$.

be inferred as NBTI characteristics even at RT.[19] Overall trends of ΔN_p and ΔD_{it} with $F_{N/O}$ were similar to those of D_{it}. After 5 min, the ΔN_p of $F_{N/O}=2$ sample was reduced to about half compared to $F_{N/O}=0$ sample. However, by more nitrogen incorporation, the NBTI characteristics were dramatically degraded. For $F_{N/O}=4$ sample, ΔN_p was three times and ΔD_{it} was ten times higher than for $F_{N/O}=2$ sample. Thus, the sample with $F_{N/O}=2$ shows the best electrical properties in terms of various key properties. These results show that the dielectric degradation can be reduced only by proper amount of nitrogen incorporation.

In addition, we carried out voltage stress measurements at elevated temperatures to investigate the degradation of dielectrics at high temperature, which is directly related to NBTI. The ΔN_p is related to stress temperature as follows:[3]

$$\Delta N_{ox} \approx A\frac{C_{ox}E_{ox}^{m}}{q}\exp\left(\frac{-E_a}{k_BT}\right)t^{\alpha}, \tag{2}$$

where C_{ox} is the gate stack capacitance per unit area, E_{ox} is electric fields, q is electron charge, and A, m, and α are constants ($m\sim3-4$, $\alpha\sim0.1-0.2$). Thus, the activation energy of positive trap charge creation (E_a) can be determined by plotting $\ln(\Delta N_p)$ as a function of $1/k_BT$. Figure 4(a) shows the Arrhenius plot of ΔN_p for HfO_2 and TMN sample prepared at $F_{N/O}=2$ between RT and 125 °C. The apparent activation energy (E_a) for the TMN samples was extracted to be 0.11 eV, which was about 40% higher than that for HfO_2 samples (0.07 eV). This increased activation energy by nitrogen incorporation results in the improvement of dielectric degradation immunity, similar to the measurements at RT shown in Fig. 3. Also, the Arrhenius plot of ΔD_{it} [Fig. 4(b)] for HfO_2 and TMN sample is obtained having the same trend with ΔN_p. The ΔD_{it} of HfO_2 has higher value and higher gradient than TMN sample.

IV. DISCUSSIONS

According to the RD model, electrical stress induces hydrogen release, generating high D_{it} and large positive charges by forming $Hf-O-Hf \equiv +Hf^{+}$.[12] Since we can expect more hydrogen release with increasing nitrogen incorporation,[20] the NBTI is expected to be enhanced with increasing nitrogen concentration, which agrees with our results for $F_{N/O}>2$. However, the improved immunity for small nitrogen incorporation cannot be explained by this simple mechanism. Previously, it was shown that the diffusion of hydrogen is slowed down by nitride layer containing small nitrogen (2%–4%) in gate oxide, resulting in the reduction in charge generation.[21,22] Thus, we propose that the trap charge generation caused by diffused hydrogen is reduced by the presence of nitrided layer, which has proper amount of nitrogen and locates away from the interface as for the TMN sample with $F_{N/O}=2$.

Schematic diagram explaining this proposition is shown in Fig. 5. For TMN sample, although we did not intentionally incorporate nitrogen to the interface, small nitrogen atoms seem to diffuse to the interface [Fig. 5(a)]. Next, the hydrogen atoms substitute Si–N and Si–O bonds at the interface during postprocess like FGA. The presence of nitrogen at the interface is expected to accelerate the incorporation of hydrogen at the interface since the activation energy of Si–N bond breaking is lower than that for Si–O bonding.[6] During CVS, more released hydrogen would generate higher D_{it} and larger positive charges. Figure 5(b) schematically shows the diffusion of released hydrogen into the bulk of gate oxide. Although these diffused hydrogen can induce dielectric degradations, nitride layer located away from the interface slows down the diffusion of released hydrogen atoms,[21,22] resulting in the reduction in the dielectric degradation. Also, this proposition is corroborated by the observation shown in Fig. 1, indicating better immunity for TMN compared to MN. In other words, relatively thicker nitrided layer of TMN prevents the hydrogen transport more efficiently than MN, producing less trap charges by voltage stress.

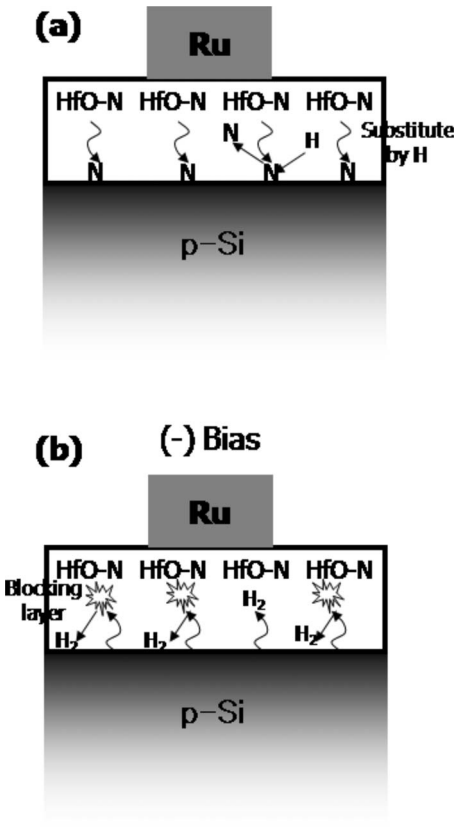

FIG. 5. Schematic drawing explains the proposed dielectric degradation mechanisms.

V. CONCLUSIONS

The NBTI characteristics of nitrogen depth profiles and concentrations in high k gate oxide were investigated. The best NBTI properties were obtained at TMN-type sample including CET of 1.10 nm and D_{it} 0.8×10^{11} cm^{-2} eV^{-1}. Also, combinatorial studies of nitrogen incorporation show that the best properties can be obtained $F_{N/O}=2$. In this case, the results of NBTI degradation with temperature show E_a of NBTI for the HfO_xN_y sample 40% higher than that of HfO_2 sample. This NBTI characteristics can be explained from blocking of hydrogen diffusion by nitrogen incorporation layer above interface based RD model. All these results clearly show that optimized NBTI properties of high k gate oxide can be obtained only by proper amount of nitrogen incorporation with designed nitrogen depth profile. Thus, the atomic scale controllability of *in situ* nitridation during PE-ALD in depth and concentration of nitrogen has great benefits compared to other nitridation processes.

ACKNOWLEDGMENTS

This work was supported by Korea Research Foundation (MOEHRD) (Grant Nos. KRF-2005-005-J13102 and KRF-2007-331-D00243) and Korea Ministry of Commerce, Industry and Energy (System IC 2010, Commercialization Program of NanoProcess Equipments). Also, this work was supported by the Korea Science and Engineering Foundation (KOSEF) (Grant Nos. R01-2007-000-20143-0 and 2007-02864). Also, Mr. Maeng was financially supported by the second stage of the Brain Korea 21 project in 2007.

[1]D. K. Schroder and J. A. Babcock, J. Appl. Phys. **94**, 1 (2003).
[2]M. Makabe, T. Kubota, and T. Kitano, IEEE 38th Annual International Reliability Physics Symposium Proceedings, 2000, pp. 205–209.
[3]M. Houssa, G. Pourtois, M. M. Heyns, and A. Stesmans, J. Phys.: Condens. Matter **17**, S2075 (2005).
[4]A. E. Islam, H. Kufluoglu, D. Varghese, S. Mahapatra, and M. A. Alam, IEEE Trans. Electron Devices **54**, 2143 (2007).
[5]S. S. Tan, T. P. Chen, J. M. Soon, K. P. Loh, C. H. Ang, and L. Chan, Appl. Phys. Lett. **82**, 1881 (2003).
[6]S. S. Tan, T. P. Chen, J. M. Soon, K. P. Loh, C. H. Ang, W. Y. Teo, and L. Chan, Appl. Phys. Lett. **83**, 530 (2003).
[7]N. Kimizuka, K. Yamaguchi, K. Imai, T. Iizuka, C. T. Liu, R. C. Keller, and T. Horiuchi, Dig. Tech. Pap. - Symp. VLSI Technol. **2000**, 92.
[8]K. Sakuma, D. Matsushita, K. Muraoka, and Y. Mitani, IEEE 44th Annual International Reliability Physics Symposium Proceedings, 2006 (unpublished), pp. 454–460.
[9]Y. Mitani, Tech. Dig. - Int. Electron Devices Meet. **2004**, 117.
[10]K. Kushida-Abdelghafar, K. Watanabe, J. Ushio, and E. Murakami, Appl. Phys. Lett. **81**, 4362 (2002).
[11]C. H. Ang, C. M. Lek, S. S. Tan, B. J. Cho, T. Chen, W. Lin, and J. Z. Zhen, Jpn. J. Appl. Phys., Part 2 **41**, L314 (2002).
[12]M. Houssa, S. De Gendt, J. L. Autran, G. Groeseneken, and M. M. Heyns, Appl. Phys. Lett. **85**, 2101 (2004).
[13]W. J. Maeng and H. Kim, Appl. Phys. Lett. **91**, 092901 (2007).
[14]E. H. Nicollian and J. R. Brews, *MOS Physics and Technology* (Wiley Interscience, New Jersey, 2003).
[15]D.-G. Park, H.-J. Cho, K.-Y. Lim, C. Lim, I.-S. Yeo, J.-S. Roh, and J. W. Park, J. Appl. Phys. **89**, 6275 (2001).
[16]T. Ino, Y. Kamimuta, M. Suzuki, M. Koyama, and A. Nishiyama, Jpn. J. Appl. Phys., Part 1 **45**, 2908 (2006).
[17]J. L. Gavartin, A. L. Shluger, A. S. Foster, and G. I. Bersuker, J. Appl. Phys. **97**, 053704 (2005).
[18]K. Xiong, J. Robertson, and S. J. Clark, J. Appl. Phys. **99**, 044105 (2006).
[19]K. Seo, R. Sreenivasan, P. C. McLntyre, and K. C. Saraswat, Tech. Dig. - Int. Electron Devices Meet. **2005**, 4.
[20]K. Onishi, C. S. Kang, R. Choi, H. J. Cho, S. Gopalan, R. Nieh, E. Dharmarajan, and J. C. Lee, Tech. Dig. - Int. Electron Devices Meet. **2001**, 659.
[21]E. Cartier, D. A. Buchanan, and G. J. Dunn, Appl. Phys. Lett. **64**, 901 (1994).
[22]T. Matsuoka, S. Taguchi, H. Ohtsuka, K. Taniguchi, C. Hamaguchi, S. Kakimoto, and K. Uda, IEEE Trans. Electron Devices **43**, 1364 (1996).